

Spin Waves and Magnetic Ordering in K_2MnF_4

R. J. Birgeneau

*Bell Laboratories, Murray Hill, New Jersey 07974
and Brookhaven National Laboratory,* Upton, New York 11973*

H. J. Guggenheim

Bell Laboratories, Murray Hill, New Jersey 07974

G. Shirane

Brookhaven National Laboratory, Upton, New York 11973*

(Received 6 November 1972)

Elastic and inelastic neutron-scattering studies of the planar antiferromagnet K_2MnF_4 have been carried out. The magnetic ordering is confirmed to be of the K_2NiF_4 type with $T_N=42.14$ K; no evidence is found for the additional $T_N=58$ K phase reported by Ikeda and Hirakawa (IH). The sublattice magnetization is found to follow a single power law over the range $6 \times 10^{-4} < 1 - T/42.14 < 3 \times 10^{-1}$, with $\beta=0.15 \pm 0.01$. This contrasts with the results of IH, who report $\beta=0.188$ up to $1 - T/T_N = 5 \times 10^{-3}$ with a crossover to three-dimensional behavior beyond $1 - T/T_N = 5 \times 10^{-3}$. The effects of a distribution of Néel temperatures on neutron order-parameter determinations is discussed, and it is shown that the apparent crossover behavior observed by IH can be accounted for on the basis of a distribution of T_N 's with standard deviation 50 mK in their crystal. The spin-wave dispersion relations in the $(q_x, 0, q_z)$ plane have been measured at 4.5 K and at T_N . The spin waves correspond precisely to those expected for a simple quadratic anisotropic Heisenberg antiferromagnet with $J_1=8.45 \pm 0.1$ K, $g\mu_B H_A=0.32$ K, and all other exchange interactions below our resolution limit. These values are in excellent accord with those determined from the susceptibility by Breed and from the sublattice magnetization and AFMR by de Wijn *et al.*, and they thence confirm that simple two-dimensional spin-wave theory gives a complete description of the low-temperature magnetic properties of K_2MnF_4 . Well-defined spin waves are observed up to T_N ; at T_N the $(q_x, 0, 0)$ dispersion relation is a simple sine wave with slope renormalized by $\approx 9\%$ from the 4.5-K value; this renormalization is correctly predicted by the $1/S$ Oguchi correction terms.

I. INTRODUCTION

Over the past several years we have reported extensive neutron scattering investigations of the magnetic behavior of the quadratic-layer (QL) antiferromagnets typified by K_2NiF_4 .¹⁻⁴ These experimental studies have been most detailed for K_2NiF_4 itself, but we have also qualitatively surveyed the magnetic ordering and fluctuation spectra of Rb_2MnF_4 and Rb_2FeF_4 . The principal result of these studies is that the K_2NiF_4 compounds have a pronounced two-dimensional (2D) character and, in particular, seem to exhibit what may be described as essentially 2D second-order magnetic phase transitions. By this we mean that the observable critical scattering is 2D at all temperatures both above and below T_N . The actual phase transition, however, is to a three dimensionally ordered state so that ultimately the critical behavior must have a three-dimensional (3D) character. This assumption to date has been that the 3D critical region is too narrow to be observed experimentally due to inhomogeneous broadening of T_N itself.

The ineffectiveness of the 3D coupling is most clearly demonstrated in Rb_2MnF_4 . In this com-

pound two magnetic phases with identical in-plane order but a different stacking of the planes exist simultaneously in the same crystal. In spite of the different 3D magnetic structures, the normalized 3D order parameters, that is, M_T/M_0 , where M_0 is the zero-degree sublattice magnetization for each phase, coincide at all temperatures. This can only be explained by assuming that the critical behavior is determined solely by the in-plane 2D properties.¹ That is, the critical behavior depends only on the in-plane Heisenberg exchange together with the magnetic dipole interaction which in this case has uniaxial-Ising symmetry thus making a conventional 2D magnetic transition allowed.¹⁻⁴

In a recent paper, Ikeda and Hirakawa⁵ (IH) have reported similar elastic and quasielastic neutron scattering studies of the isomorphous compound K_2MnF_4 . Their results, in general, parallel closely our observations in the other quadratic layer antiferromagnets. However, there are two intriguing and possibly quite important differences. Firstly, they observe two different 3D magnetic structures as in Rb_2MnF_4 but in their case the Néel temperatures for the two phases differ by more than 35%. This would necessitate that the

3D coupling play an essential role for at least one of the two phases. Secondly, in the K_2NiF_4 -type magnetic phase of K_2MnF_4 , IH apparently observe a distinct changeover from 2D to 3D critical behavior in the order parameter at $\tau = 1 - T/T_N \sim 5 \times 10^{-3}$. No such changeover was observed in K_2NiF_4 itself although anomalous behavior was found in Rb_2FeF_4 .¹ Both of these results have important consequences for our understanding of these quadratic layer antiferromagnets.⁶ It seemed worthwhile therefore to repeat the IH experiments in our samples in order to elucidate their results.

There is also considerable interest in *inelastic* neutron scattering studies of K_2MnF_4 . Rather complete information is now available on the magnetic properties of K_2MnF_4 including the susceptibility,^{7,8} specific heat,⁹ zero-point spin deviation,¹⁰ and sublattice magnetization.¹¹ The low-temperature susceptibilities have been analyzed in detail by Breed⁶ using spin-wave theory including Oguchi's correction terms.¹² The sublattice magnetization has similarly been analyzed in an accompanying paper by de Wijn, Walker, and Walstedt¹³ with results essentially identical to those of Breed for the interaction constants. In order to complete the picture and to confirm unambiguously the accuracy of spin-wave theory for the low-temperature thermodynamic properties, it is essential to have a direct measurement of the spin-wave dispersion relations themselves. Finally, K_2MnF_4 supplies the possibility of a test of theory for spin-wave interaction effects in two dimensions. The calculations of Breed and de Wijn *et al.* using Oguchi's $1/S$ expansion¹² indicate that near T_N there should be approximately a 9% renormalization of the magnon energies. This should be readily observable in the neutron scattering spectra. As discussed by de Wijn *et al.*, it has already been observed that renormalized spin-wave theory is only capable of describing the thermodynamic magnetic properties up to $\sim \frac{1}{2} T_N$. A corresponding test of Oguchi's theory for the spin-wave energies themselves should therefore be quite informative.

II. ELASTIC NEUTRON SCATTERING

The elastic neutron scattering experiments were performed on a two-axis spectrometer at the Brookhaven high flux beam reactor (HFBR). Neutrons of wavelength 1.252 Å were obtained by reflection from the (311) plane of a germanium monochromator. The K_2MnF_4 crystal was a flat plate $1 \times 4 \times 12$ mm³ with the c axis perpendicular to the plate face. The crystal was grown using the horizontal-zone-melting method described previously.¹ The sample was mounted with its [110] crystallographic axis (which corresponded to the long axis of the crystal), vertical on an aluminum pedestal using a thin layer of Hysol Epoxy type 1C; both the

pedestal and glue were covered with cadmium. The sample holder was then mounted in a Cryogenics Associates temperature-control Dewar. Around 40 K relative temperatures were found to be reproducible to within 0.010 K.

The magnetic structure of K_2MnF_4 was first studied by Loopstra *et al.*¹⁴ using powder neutron-diffraction techniques. They found that at 4.2 K, K_2MnF_4 has the K_2NiF_4 -type magnetic structure¹⁵ illustrated in Fig. 1. This structure is orthorhombic with simple square antiferromagnetic layers stacked such that next-nearest-neighbor (nnn) plane spins along the c axis are parallel. The nearest-neighbor (nn) planes are uncorrelated so that in a single crystal with the [110] chemical axis vertical, separate [010] and [100] magnetic domains appear as illustrated in the reciprocal-lattice diagram of Fig. 1.

As discussed in the Introduction, single-crystal magnetic structure studies of K_2MnF_4 were carried out by Ikeda and Hirakawa.⁵ They found that intense Bragg scattering appeared at the positions (100), (011), (102), etc. at $T = 42.37$ K. This temperature should be compared with the $T_N = 45$ K deduced by Breed⁷ from susceptibility measurements and $T_N = 42.1$ K found by Salamon and Ikeda⁹ from the specific heat. However, IH also found additional magnetic Bragg scattering at the positions $(10\frac{1}{2})$, $(10\frac{3}{2})$ which appeared at 58 K. They identified these latter Bragg peaks with a second magnetic phase having the Ca_2MnO_4 -type magnetic structure¹⁶ with nnn plane c -axis spins antiparallel. This second phase, ordering at 58 K, has not been detected by other workers. Finally, IH found that

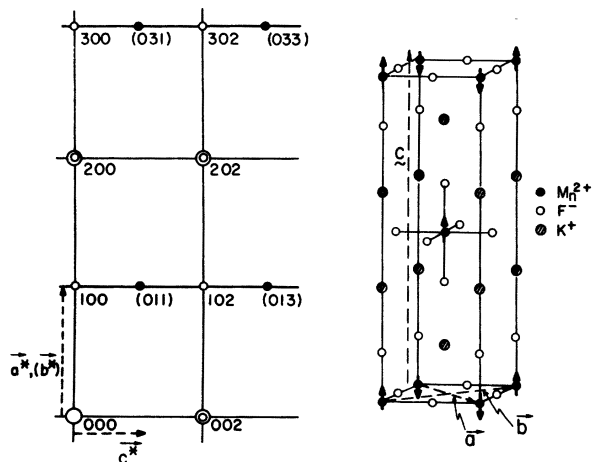


FIG. 1. Chemical and magnetic structure of K_2MnF_4 . Inverting the central spin exchanges the a and b axes. The reciprocal lattice displays both the [010] and [100] magnetic zones. Nuclear Bragg peaks are indicated by double circles. Around $T_N = 42.14$ K, $a^* = 1.068$ Å⁻¹, $c^* = 0.4741$ Å⁻¹.

when the (100) intensity, with background suitably removed, was plotted on log-log paper versus $\tau = 1 - T/42.37$, there were two distinct linear regions: $\tau \sim 1$ to 5×10^{-3} where $\beta = 0.19$, and $\tau \sim 5 \times 10^{-3}$ to 3×10^{-4} where $\beta \gtrsim 0.3$.

The results of our own study may be very briefly stated. We observe magnetic Bragg scattering only at the K_2NiF_4 -type positions. More precisely, at $T = 34$ K any Bragg scattering at the $(10\frac{1}{2})$ position is at most 10^{-4} of that at (100). This may be compared with the IH result of 10^{-1} . We conclude therefore that the $T_N = 58.0$ K phase is confined to the IH crystal alone. We assume that it originates in a second *chemical* phase; however, this problem can only be elucidated by further chemical and magnetic research on the part of IH.

We have also carried out a cursory study of the magnetic Bragg and 2D magnetic critical scattering intensities as a function of temperature. Our results are in general in good agreement with those of IH but with some important differences. The critical scattering, which has the form of a ridge along the c axis, peaks at $T^* = 42.15 \pm 0.015$ K compared with the IH value of 42.37 K. The ridge peak is highly asymmetric in temperature dropping off much more rapidly below than above; this same behavior was observed in K_2NiF_4 (Ref. 3) and is assumed to be characteristic of 2D phase transitions. As discussed in the Appendix, for the 2D Ising model this asymmetry factor is 37.¹⁷

In the absence of extinction effects, etc., the (100) Bragg intensity is simply proportional to the square of the sublattice magnetization so that in the critical region one expects

$$I_T/I_0 \propto (M_T/M_0)^2 = B^2 (1 - T/T_N)^{2\beta}. \quad (1)$$

Unfortunately, our intensity data are somewhat sparse since the experiment was carried out originally as simply a check on IH. However, even with our limited data there is a clear difference from IH very close to 42.15 K in that we see *no apparent crossover*. This crossover effect is discussed extensively in the Appendix, where it is shown that simple inhomogeneous broadening of T_N may cause an apparent changeover in β . For the 2D Ising model, the crossover point is 3.5σ , where σ is the standard deviation for a Gaussian spread in T_N and the apparent T_N is located by the peak in the staggered susceptibility. The IH crossover at $1 - T/T_N = 0.19$ K, therefore, would imply $\sigma = 0.05$ K, a highly plausible number.

As discussed in the Appendix, if one assumes that the true order parameter follows a single power up to at least σ/T_N in reduced temperature, then the intrinsic β and T_N may be obtained by simple least-squares fits to the data up to $\sim T_N - 2\sigma$. Attempts to fit data within the 2σ region of smearing produced a marked increase in the χ^2 of the fit.

Results of such fits to our data for $1 - T/T_N < 10^{-1}$ are shown in Fig. 2. We obtain a good fit to a single power law down to at least $1 - T/T_N < 6 \times 10^{-4}$ with $\beta = 0.15 \pm 0.01$ and $T_N = 42.14$ K. The fitted T_N lies satisfactorily close to the ridge-peak-intensity temperature of 42.15 ± 0.015 K indicating that the spread in T_N in our sample is in fact not a serious problem. This value of β may be compared with the values 0.138 ± 0.004 and 0.16 ± 0.01 found in K_2NiF_4 (Ref. 3) and Rb_2MnF_4 ,¹ respectively.

III. INELASTIC NEUTRON SCATTERING

The inelastic experiments were carried out on the H7 triple-axis spectrometer at HFBR. All measurements were carried out in the constant- Q mode of operation with incoming neutrons of energy 13.5 meV. Pyrolytic graphite (002) planes were used for both monochromator and analyzer with the monochromator crystal bent about a horizontal axis to provide focusing of the incident neutrons.¹⁸ A large mosaic pyrolytic graphite crystal placed before the sample acted as a tuned $\frac{1}{2}\lambda$ filter.¹⁹ Horizontal collimation was typically 40 min throughout except for the before-sample collimator which was kept at 20 min. The vertical collimation was determined by the height of the sample and the collimators and was therefore quite loose.

Spin-wave theory for K_2MnF_4 , including the Oguchi $1/S$ corrections,¹² has been discussed in detail by Breed⁸ and more recently by de Wijn *et al.*¹³ Writing the Hamiltonian

$$\mathcal{H} = \sum_i g\mu_B H_A S_i^z + \sum_{i>j} J_{ij} \vec{S}_i \cdot \vec{S}_j, \quad (2)$$

then at $q = 0$

$$E(0) \approx [8(J_1 + J'_1)Sg\mu_B H_A]^{1/2} \quad (3)$$

and for $\vec{q} = (q_x, 0, q_x)$ away from $q_x = 0$

$$E(q_x, 0, q_x) \approx 4J_1 S \left| \sin \frac{1}{2} q_x a \right| (1 - J_2/J_1) \times [1 + (J'_1/J_1) \cos \frac{1}{2} q_x c] \quad (4)$$

for $g\mu_B H_A$, $J'_1, J_2 \ll J_1$. Here J_1 and J_2 are, respectively, the nn and nnn *in-plane* exchange constants and J'_1 is the nn *between-plane* exchange. The anisotropy is predominantly dipolar in origin, but for our purposes here it may be adequately represented by the anisotropy field H_A . The dispersion relation for $\vec{q} = (0, q_y, q_x)$ is obtained from Eq. (4) by replacing q_x by q_y and omitting the J'_1/J_1 term.²

Following Keffer,²⁰ the higher-order $1/S$ correction terms as calculated by Oguchi may be simply included in Eq. (4) for the in-plane magnons by letting

$$J_1 \rightarrow J_1 [1 - i(T)] , \quad (5)$$

where

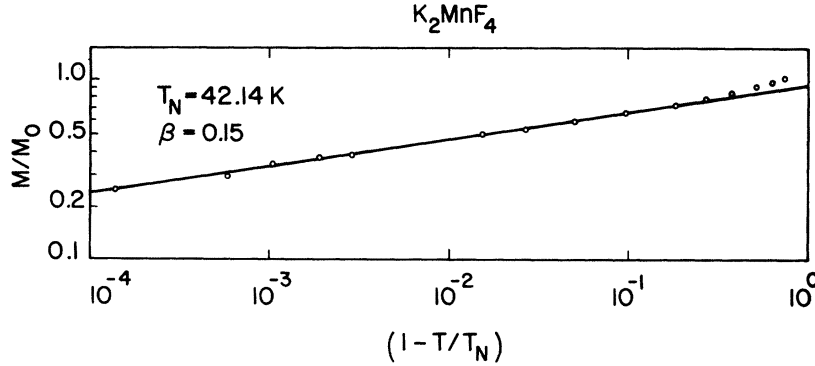


FIG. 2. Reduced sublattice magnetization in K_2MnF_4 as a function of reduced temperature. The solid line is the best fit to the data of a single power law with $T_N = 42.14$ K, $\beta = 0.15$.

$$\chi(T) = -\frac{0.632}{8S} + \frac{1}{N_0S} \sum_q \langle n_q \rangle \frac{1 + \alpha - \cos^2 \frac{1}{2} q_x a \cos^2 \frac{1}{2} q_y a}{(1 + \alpha)^2 - \cos^2 \frac{1}{2} q_x a \cos^2 \frac{1}{2} q_y a}$$

and where $\alpha = g\mu_B H_A / 4SJ_1$ is chosen empirically so as to give the observed temperature dependence of the gap.²¹ All terms of the order of J_2/J_1 , J'_1/J_1 have been omitted in Eq. (5). From the low-temperature perpendicular susceptibility using Oguchi-type spin-wave theory Breed has deduced $J_1 = 8.40 \pm 0.10$ K and from the spin-flop field $g\mu_B H_A$

$= 0.32$ K. de Wijn *et al.* in the previous paper have found values in essential agreement with these. Both groups assume that J_2 and J'_1 are negligible.

Typical experimental results are shown in Figs. 3 and 4. Because of the small volume of the sample, rather long counting times had to be used, particularly for excitations at elevated temperatures near the zone boundary. From Figs. 3 and 4 it may be seen that the spin waves remain well defined right up to T_N although they do broaden more rapidly than those in K_2NiF_4 .^{2,4} The consequent dispersion relations in the directions $(\zeta_x a^*, 0, 0)$ and $(0, 25a^*, 0, \zeta_x c^*)$ [plus $(q_x \leftrightarrow q_y)$] are shown in Fig. 5.

We consider firstly the results at 4.5 K. For the 4.5 K gap we find $E_0 = 0.65 \pm 0.05$ meV = 7.5

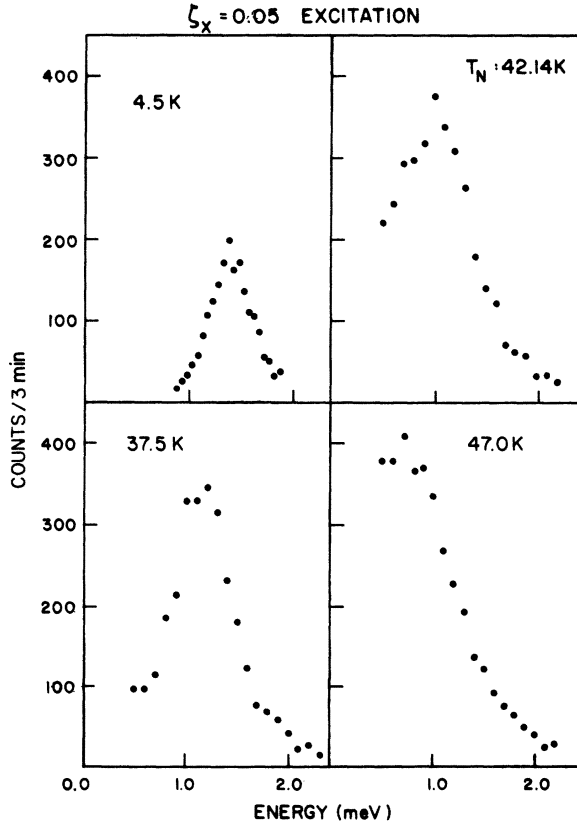


FIG. 3. Inelastic scattering as a function of temperature at the position $(0.05a^*, 0, 0.6c^*)$.

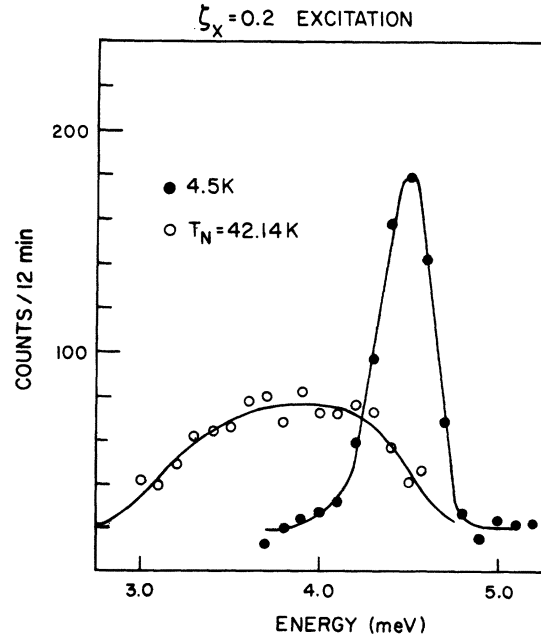


FIG. 4. Spin-wave scattering at 4.5 K and $T_N = 42.14$ K at the position $(0.2a^*, 0, 0.6c^*)$. The solid lines are merely guides to the eye.

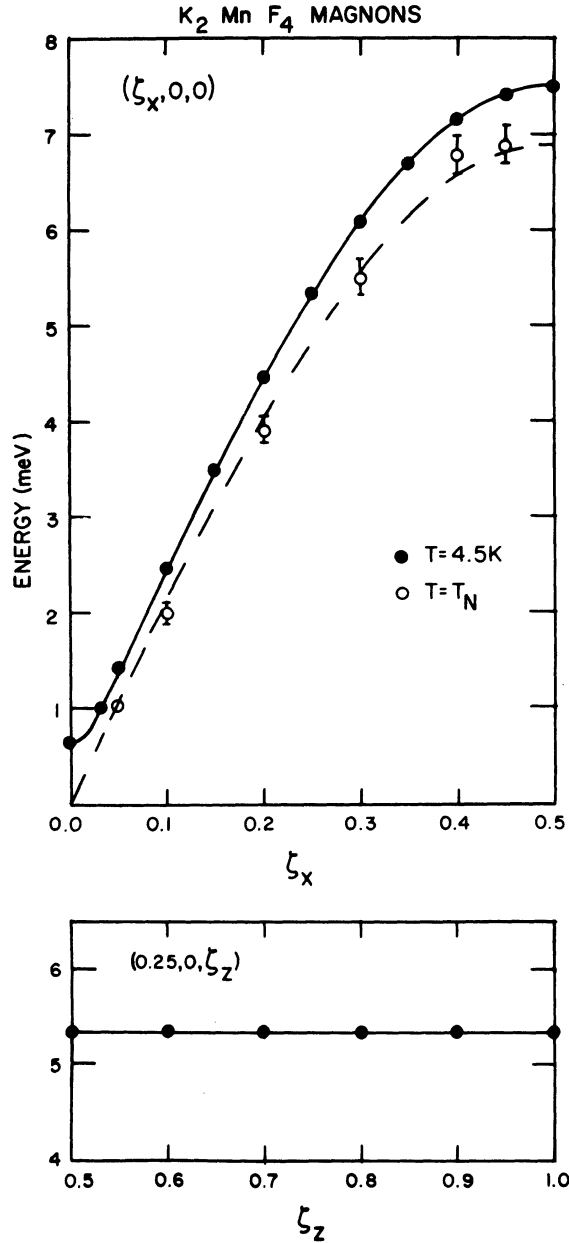


FIG. 5. Spin-wave dispersion relations in K_2MnF_4 at 4.5 K and at T_N in the directions $(\xi_x, a^* 0, 0)$ and $(0.25a^*, 0, \xi_z c^*)$.

± 0.6 K in good agreement with the AFMR value of 7.40 ± 0.05 K. We shall use this latter value in our fits since it is considerably more accurate. It is apparent that as in K_2NiF_4 there is no measurable dispersion in the c direction to within experimental error. This necessitates that $|J'_1/J_1| < 1/250$, thus confirming the essential two-dimensionality of the magnetism. It should be emphasized that J'_1 measures the strength between nearest-neighbor planes whereas it is the coupling between next-nearest-

neighbor planes which determines the 3D order. de Wijn *et al.*,¹³ from their NMR measurements, have put an upper limit of $4 \times 10^{-4} J_1$ on this nnn plane interaction. This is consistent with our measurement of $J'_1 < 4 \times 10^{-3} J_1$, given the increased number of ligands involved in any superexchange path between nnn planes. Thus the actual 3D ordering pattern is determined by a balance between the long-range magnetic dipole interaction and this very weak nnn plane exchange.

The solid line in Fig. 5 represents a least-squares fit of the full expression for the dispersion relation to the measured in-plane dispersion curve at 4.5 K. The best-fit parameters are

$$\begin{aligned} J_1^s &= 8.72 \pm 0.10 \text{ K}, \\ J_2^s &\sim 0.00, \\ g\mu_B H_A^s &= 0.317 \pm 0.004 \text{ K}, \end{aligned} \quad (6)$$

where the superscript s implies that these are obtained from fits to simple spin-wave theory without the fourth-order Oguchi corrections. The correlation between J_1^s and J_2^s in the fit is 98%, so we can only say with absolute confidence that $J_1^s - J_2^s = 8.72 \pm 0.1$ K and that J_2^s is too small to be determined from the $(\xi_x, 0, \xi_z)$ dispersion curves. This situation was also encountered in the case of K_2NiF_4 .

As discussed previously, the zero-point Oguchi corrections may be simply included by letting $J_1 = J_1^s / [1 - i(0)]$. Thus we have finally

$$\begin{aligned} J_1 &= 8.45 \pm 0.10 \text{ K}, \\ J_2 &\sim 0.00, \\ g\mu_B H_A &= 0.317 \pm 0.004 \text{ K}. \end{aligned} \quad (7)$$

These should be compared with the values $J_1 = 8.40 \pm 0.10$, $g\mu_B H_A = 0.32$ K deduced by Breed from the low-temperature susceptibility and spin-flop field and $J_1 = 8.41 \pm 0.06$ K, $g\mu_B H_A = 0.32$ K deduced by de Wijn *et al.* from the sublattice magnetization and the AFMR. The agreement is clearly excellent. We conclude, therefore, that simple spin-wave theory including the first $1/S$ correction terms successfully describes all of the low-temperature magnetic properties of K_2MnF_4 .

Using the Oguchi theory, we may also calculate the renormalization of the spin-wave dispersion curve as a function of temperature. Such a calculation has, in fact, already been carried out by de Wijn²² using the parameters appropriate to K_2MnF_4 . He finds that at $T_N = 42.14$ K the second term in $i(T)$ in Eq. (5) has the value $+0.089$. The dispersion relation at T_N , therefore, should be a simple sine curve with zone boundary energy $E(0.5, 0, 0) = 4 \times \frac{5}{2} \times 8.45 (1 + 0.0316 - 0.089) = 80$ K $= 6.9$ meV. The appropriate curve is shown as the dotted line in Fig. 5. Again the agreement be-

tween experiment and theory is excellent. Thus, Oguchi's $1/S$ expansion theory properly describes the renormalization of the spin-wave energies right up to T_N in this quadratic layer antiferromagnet. Corresponding theory for the spin-wave lifetimes would clearly be of considerable interest.

IV. CONCLUDING REMARKS

In summary, therefore, from our elastic scattering measurements, we find that K_2MnF_4 has the K_2NiF_4 -magnetic structure with $T_N = 42.14$ K. We find no evidence in our sample for the second phase with $T_N = 58$ K observed by Ikeda and Hirakawa. The sublattice magnetization is found to follow a simple power law for $1 - T/42.14 < 10^{-1}$ with $\beta = 0.15 \pm 0.01$. We find no evidence for a crossover effect to 3D critical behavior; instead it has been shown that the apparent crossover observed by IH could result simply from a distribution of Néel temperatures with standard deviation 0.05 K in their sample.

From the inelastic measurements it is found that simple spin-wave theory is remarkably successful in describing the low-temperature magnetic properties of K_2MnF_4 . The interaction parameters deduced by Breed from the spin-flop field and χ_L are found to reproduce the measured spin-wave dispersion curves both at 4.5 K and at T_N itself, provided that Oguchi $1/S$ renormalization effects are included. As noted previously, spin-wave theory for the sublattice magnetization breaks down at $\sim \frac{1}{2}T_N$. Our results show clearly, therefore, this breakdown is not due to an intrinsic error in the spin-wave part but rather to the neglect of other contributions, notably the longitudinal critical fluctuations.

The spin waves in K_2MnF_4 show clearly the effects of spin-wave renormalization by the energy rather than the magnetization.²³ As discussed previously in the context of K_2NiF_4 , the characteristic feature of these 2D near-Heisenberg systems is that the near-neighbor correlations remain anomalously strong even above T_N . This is apparent in $\chi(\vec{Q})$,^{4,5} in the specific heat,⁹ and in the NMR linewidths.²⁴ These enhanced correlations are directly related to the fact that T_N is much smaller than T_{MF} , the molecular field ordering temperature, and correspondingly $k_B T_N$ is $\sim 5/S$ times smaller than the zone boundary magnon energy. Thus near T_N only relatively long-wavelength magnons are appreciably populated and the consequent spin-wave interaction effects are small. This situation is even more dramatically illustrated in 1D systems such as $(CD_3)_4N MnCl_3$ where sharp spin-wave excitations are observed over a wide range of temperature in the complete absence of long-range order.²⁵

Finally, we should comment briefly on the na-

ture of the phase transition in K_2MnF_4 . As is well known, Stanley and Kaplan²⁶ showed that series expansions indicate that a 2D Heisenberg antiferromagnet will have a divergent staggered susceptibility at a temperature given to within a few percent by

$$k_B T_c^{(2)} = \frac{1}{10} J(Z-1) [2S(S+1) - 1]. \quad (8)$$

The nature of the magnetic state below $T_c^{(2)}$ has been the subject of extensive discussion in the literature since there is an exact proof for the Heisenberg model that there can be no long-range order above $T=0$.²⁷ The subtle nuances involved in this problem, however, are not relevant to K_2MnF_4 since, as we have seen, there is an Ising-type anisotropy term which stabilizes a conventional long-range ordered state. For K_2MnF_4 $Z=4$, $S=\frac{5}{2}$, $J=8.45$ K giving $T_c^{(2)}=41.8$ K compared with $T_N=42.14$ K. Thus, Eq. (8) does give an accurate estimate of the temperature at which the staggered susceptibility becomes sufficiently large that the anisotropy field, $g\mu_B H_A = 0.32$ K, can induce long-range order. The identical situation occurs in K_2NiF_4 where $T_c^{(2)}=93.1$ K and $T_N=97.1$ K.²⁸ We should also emphasize that since the critical scattering is always ridgelike, it seems to be the anisotropy rather than any 3D coupling which drives the phase transition. This is again consistent with our measurements and those of de Wijn *et al.* which indicate that $g\mu_B H_A$ is much larger than nnn plane coupling. The reader is referred to the work on K_2NiF_4 ¹⁻⁴ for a more extensive discussion of the ordering process in these materials.

ACKNOWLEDGMENTS

We should like to thank P. A. Lindgard for a number of helpful conversations on this work and for a critical reading of the manuscript. We should also like to thank H. W. de Wijn, L. R. Walker, and R. E. Walstedt for communicating their results prior to publication and for stimulating discussions on the properties of K_2MnF_4 .

APPENDIX: EFFECT OF INHOMOGENEITIES ON APPARENT ORDER PARAMETER

In this paper and in our previous work on the K_2NiF_4 -type quadratic-layer antiferromagnets, it has been emphasized that even though the phase transition is 3D, the fluctuation behavior seems to be entirely 2D in character. There must, however, be some finite range of temperature near the phase transition where the critical behavior does indeed change over and become 3D. This might be particularly evident in the order parameter exponent β , which should go from $\sim \frac{1}{8}$ to $\sim \frac{1}{3}$. In K_2NiF_4 itself, no such changeover is observed and instead, it has been suggested that the 3D critical region is too narrow to observe. However, both in Rb_2FeF_4

and in the work of Ikeda and Hirakawa in K_2MnF_4 , two distinct regions near and far from T_N , characterized by high and low β 's, respectively, are apparently observed. The concomitant kink occurs at $1 - T/T_N = 5 \times 10^{-3}$ and 1.5×10^{-2} in K_2MnF_4 and Rb_2FeF_4 , respectively. In the Rb_2FeF_4 paper, however, it is suggested on a heuristic basis alone that this changeover could "arise either from a fundamental change in the critical behavior or else from an extraneous effect such as a distribution of

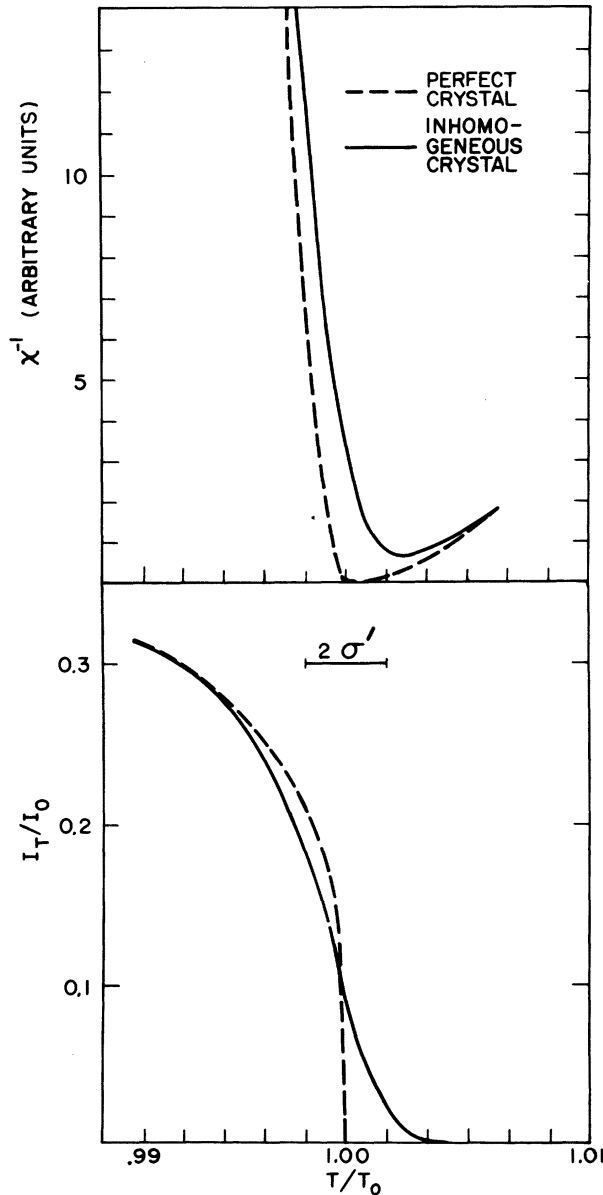


FIG. 6. Effective inverse susceptibility χ^{-1} and effective magnetic Bragg scattering for a perfect crystal and for an inhomogeneous crystal with a Gaussian distribution of Néel temperatures with standard deviation $\sigma' = \sigma/T_0 = 0.002$.

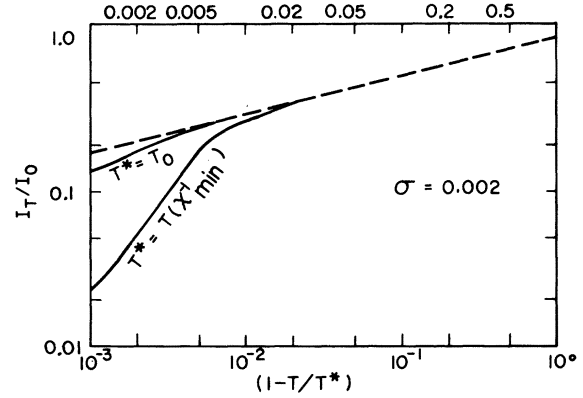


FIG. 7. Solid lines are the intensity results of Fig. 6 plotted on log-log paper vs reduced temperature with $T^* = T(\chi_{\min}^{-1})$, the temperature at which χ^{-1} has its minimum value, and $T^* = T_0$, the mean of the Gaussian distribution for the inhomogeneous crystal. The dotted line is the corresponding curve for the perfect crystal.

Néel temperatures." The effect of a distribution of critical temperatures has already been considered in some detail for the specific heat in liquid-gas systems,²⁹ superfluid helium,³⁰ and in certain magnetic systems. We now consider the corresponding effects on the apparent order parameter in these pseudo-2D magnets.

For simplicity we assume that the bulk sample is composed of a collection of microcrystals with a Gaussian distribution of ordering temperatures, that is

$$f(T_N) = \frac{1}{\sqrt{2\pi}\sigma} \exp\left[-\frac{1}{2}\left(\frac{T_N - T_0}{\sigma}\right)^2\right], \quad (A1)$$

with mean T_0 and standard deviation σ . For computational purposes we assume

$$I_T/I_0 = (M_T/M_0)^2 = (1 - T/T_N)^{0.25} \quad \text{for } T \leq T_N \\ = 0 \quad \text{for } T > T_N, \quad (A2)$$

$$\chi^{-1} = 37(1 - T/T_N)^{1.75} \quad \text{for } T < T_N \\ = (T/T_N - 1)^{1.75} \quad \text{for } T > T_N, \quad (A3)$$

so that $\beta = 0.125$, $\gamma = \gamma' = 1.75$, and the asymmetry in the susceptibility is a factor of 37 as in the 2D Ising model.¹⁷ We have chosen to consider χ^{-1} rather than χ since this is rather easier to handle computationally. The experimentally observed quantities for a system described by Eqs. (A2) and (A3) may be readily obtained by numerical convolution with the distribution function Eq. (A1). Typical numerical results for $\sigma = 0.002T_0$ are shown in Fig. 6. As expected, there is considerable rounding in I_T/I_0 . More importantly, however, the minimum in χ^{-1} is drastically shifted to higher temperatures, by about 1.5σ , owing to the factor 37 in Eq. (A3) for $T < T_N$.

The difficulty involved in analyzing data of the form shown in Fig. 6 is immediately apparent. The conventional approach in neutron diffraction experiments, and in fact that taken for Rb_2FeF_4 by us and for K_2MnF_4 by IH is to identify $T(\chi_{\max})$ as T_N and then to plot the intensity versus $1 - T/T_N$ on log-log paper. In a real experiment, of course, one actually measures $\chi(\vec{Q})$ convoluted with the instrumental resolution function and finds the maximum in this quantity at some \vec{Q} . For illustrative purposes here, however, this process can be approximated by taking $T_N = T(\chi_{\min}^{-1})$.

The consequences of this technique are clearly illustrated in Fig. 7. The apparent order parameter has two distinct regions with low and high β 's simulating precisely a changeover from two- to three-dimensional critical behavior! This apparent changeover sets in at about 3.5 σ . In the IH K_2MnF_4 crystal this would imply $\sigma \sim 50$ mk, an entirely reasonable number, given that their T_N and ours differ by about 300 mk. It is clear, therefore, that true 3D behavior for the order parameter in these K_2NiF_4 -type compounds can only be observed in relatively perfect crystals; in all probability to date only the effects of inhomogeneities have been observed.

Nevertheless, it is still possible to obtain an accurate value for β provided that the true order parameter obeys a single power law over at least one decade outside of the region $1 - T/T_N > \sigma$. As an illustration, we give in Table I results of least-squares fits to the intensity data of Fig. 6 as a

TABLE I. Results of least-squares fits of convoluted intensity data with $\sigma = 0.002T_0$ to the power law $I_T/I_0 = D(1 - T/T_N)^{2\beta}$.

T_{cutoff}/T_0	β	T_N/T_0	$\langle \%D_{\text{err}} \rangle$
0.994	0.125	0.9997	0.07
0.996	0.124	0.9993	0.36
0.998	0.121	0.9988	0.69
1.000	0.14	1.0001	7.0

function of the cut-off temperature. From the table it is apparent that both β and T_N are given accurately for reduced temperature values down to 2σ and the breakdown of the power-law description beyond this point owing to the spread in T_N manifests itself clearly in the chi square. The converse situation, however, is much more difficult to treat, particularly if one relies on neutron scattering measurements alone. In order to demonstrate convincingly that an intrinsic changeover in critical behavior has occurred, one would have to prove that the σ characterizing the sample is at least an order of magnitude less than the reduced crossover temperature. This might be effected by observing the rounding of the specific heat, but it is clearly a nontrivial task. Finally, we should note that similar "crossover" effects may also be observed if there is a temperature gradient across the sample. However, this can easily be checked experimentally by observing the temperature dependence of the order parameter in different parts of the sample via suitable masking.

*Work at Brookhaven performed under the auspices of the U.S. Atomic Energy Commission.

¹R. J. Birgeneau, H. J. Guggenheim, and G. Shirane, Phys. Rev. Lett. **22**, 720 (1969); Phys. Rev. B **1**, 2211 (1970).

²J. Skalyo, Jr., G. Shirane, R. J. Birgeneau, and H. J. Guggenheim, Phys. Rev. Lett. **23**, 1394 (1969).

³R. J. Birgeneau, J. Skalyo, Jr., and G. Shirane, J. Appl. Phys. **41**, 1303 (1970).

⁴R. J. Birgeneau, J. Skalyo, Jr., and G. Shirane, Phys. Rev. B **3**, 1736 (1971).

⁵H. Ikeda and K. Hirakawa, J. Phys. Soc. Jap. **33**, 393 (1972)

⁶For a discussion of the effects of "lattice anisotropy" on critical behavior see, for example, Gerald Paul and H. Eugene Stanley, Phys. Rev. B **5**, 2578 (1972), and references contained therein.

⁷D. J. Breed, Physica (Utr.) **37**, 35 (1967).

⁸D. J. Breed, thesis (University of Amsterdam, 1969) (unpublished).

⁹M. B. Salamon and H. Ikeda, Phys. Rev. B **7**, 2017 (1973).

¹⁰R. E. Walstedt, H. W. de Wijn, and H. J. Guggenheim, Phys. Rev. Lett. **25**, 1119 (1970).

¹¹H. W. de Wijn, R. E. Walstedt, L. R. Walker, and H. J. Guggenheim, Phys. Rev. Lett. **24**, 832 (1970).

¹²T. Oguchi, Phys. Rev. **117**, 117 (1960).

¹³H. W. de Wijn, L. R. Walker, and R. E. Walstedt, first preceding paper, Phys. Rev. B **8**, 285 (1973).

¹⁴B. O. Loopstra, B. van Laar, and D. J. Breed, Phys. Lett. A **26**, 526 (1968); Phys. Lett. A **27**, 188 (E) (1968).

¹⁵E. Legrand and R. Plumier, Phys. Status Solidi **2**, 317

(1962).

¹⁶D. E. Cox, G. Shirane, R. J. Birgeneau, and J. B. Mac Chesney, Phys. Rev. B **1**, 2211 (1970).

¹⁷For a review, see M. E. Fisher, Rep. Prog. Phys. **30**, 615 (1967).

¹⁸T. Riste, Nucl. Instrum. Methods **86**, 1 (1970); A. C. Nunes and G. Shirane, Nucl. Instrum. Methods **95**, 445 (1971).

¹⁹G. Shirane and V. J. Minkewicz, Nucl. Instrum. Methods **89**, 109 (1970).

²⁰F. Keffer, in *Handbuch der Physik*, edited by S. Flügge (Springer, Berlin 1962), Vol. XVIII/2, p. 1.

²¹H. W. de Wijn, L. R. Walker, S. Geschwind, and H. J. Guggenheim, second preceding paper, Phys. Rev. B **8**, 299 (1973).

²²H. W. de Wijn (private communication).

²³F. Keffer and R. Loudon, J. Appl. Phys. Suppl. **32**, 2S (1961); J. Appl. Phys. **33**, 250 (1962).

²⁴E. P. Maarschall, A. C. Batterman, S. Vega, and A. R. Midiema, Physica (Utr.) **41**, 473 (1969).

²⁵M. T. Hutchings, G. Shirane, R. J. Birgeneau, and S. L. Holt, Phys. Rev. B **5**, 1999 (1972).

²⁶H. E. Stanley and T. A. Kaplan, Phys. Rev. Lett. **17**, 913 (1966). H. E. Stanley, J. Appl. Phys. **40**, 1546 (1969).

²⁷P. C. Hohenberg, Phys. Rev. **158**, 383 (1967); N. D.

Mermin and H. Wagner, Phys. Rev. Lett. **17**, 1133 (1966).

²⁸For an extensive tabulation of $T_c^{(2)}$ and T_N in a variety of planar antiferromagnets, see L. J. de Jongh, P. Bloembergen, and J. H. P. Colpa, Physica (Utr.) **58**, 305 (1972).

²⁹P. C. Hohenberg and M. Barmatz, Phys. Rev. A **6**, 289 (1972).

³⁰Guenter Ahlers, Phys. Rev. **171**, 275 (1968).